Energy Materials

Supplementary Materials

Graphdiyne-enabled interfacial transport sieving for efficient and sustainable carbon-based perovskite photovoltaics

Haochun Sun[1,2,#], Wenqiang Fan[1,2,#], Chenzhe Xu[1,2,#], Yingcong Liu[1,2], Hongwei Wang[1,2], Liyan Hu[1,2], Zhuojian Liang[1,2,*], Linkai Yu[1,2], Yijian Lu[1,2], Zhuo Kang[1,2,*], Yue Zhang[1,2,*]

[1]Academy for Advanced Interdisciplinary Science and Technology, Beijing Key Laboratory for Advanced Energy Materials and Technologies, State Key Laboratory for Advanced Metals and Materials, University of Science and Technology Beijing, Beijing 100083, China.
[2]School of Materials Science and Engineering, Key Laboratory of Advanced Materials and Devices for Post-Moore Chips Ministry of Education, University of Science and Technology Beijing, Beijing 100083, China.
[#]These authors contributed equally to this work.

[*]**Correspondence to:** Prof. Zhuojian Liang, Prof. Zhuo Kang, Prof. Yue Zhang, Academy for Advanced Interdisciplinary Science and Technology, Beijing Key Laboratory for Advanced Energy Materials and Technologies, State Key Laboratory for Advanced Metals and Materials, University of Science and Technology Beijing, Beijing 100083, China; School of Materials Science and Engineering, Key Laboratory of Advanced Materials and Devices for Post-Moore Chips Ministry of Education, University of Science and Technology Beijing, Beijing 100083, China. E-mail: zjliang@ustb.edu.cn; zhuokang@ustb.edu.cn; yuezhang@ustb.edu.cn

Supplementary Note

Supplementary Note 1: Pb^{2+} sorption kinetics of GDY

GDY (20 mg) was added to 50.0 mL of an aqueous Pb^{2+} solution with an initial concentration of 10.0 ppm in a 100-mL beaker and stirred at room temperature. During the sorption process, aliquots were collected at selected time points (0, 0.1, 0.2, 0.4, 0.8, 2, 3, 5, 7.5, 10, 13, and 16 h), filtered through a 0.22-μm membrane filter, and diluted with deionized water before ICP-MS analysis of the residual Pb^{2+} concentration. The corresponding residual Pb^{2+} concentrations at these time points were 10.0000, 8.8740, 7.9872, 6.9312, 4.7859, 1.0532, 0.4941, 0.3549, 0.5643, 0.4332, 0.4076, and 0.3482 ppm, respectively. To quantitatively describe the rapid decrease in Pb^{2+} concentration during the initial sorption stage, the first six data points were empirically fitted using an apparent first-order concentration-decay model:

$$\ln\left(\frac{C_t}{C_0}\right) = -k_{app}t \qquad (S1)$$

where C_0 and C_t are the Pb^{2+} concentrations in solution at t=0 and time t, and k_{app} is the apparent first-order rate constant. Linear fitting of the initial sorption regime yields k_{app} = 1.12 h^{-1} [Figure 4D, inset]. This empirical parameter is used to characterize the initial rate of Pb^{2+} removal from solution rather than to assign a specific microscopic adsorption mechanism.

The affinity of GDY toward Pb^{2+} was further described using the distribution coefficient (K_d):

$$K_d = \frac{\text{Pb(II) sorbed on sorbents (mg g}^{-1})}{\text{Pb(II) in solution (mg mL}^{-1})} = \frac{(\mathrm{C_i} - \mathrm{C_f})V}{\mathrm{C_f}m} \quad (S2)$$

where C_i is the initial Pb concentration, C_f refers to the equilibrium Pb concentration, V is the solution volume, and m is the mass of GDY. The calculated K_d value is 6.93×10^4 mL g^{-1}.

Supplementary Note 2: Pb^{2+} sorption isotherm of GDY

Aqueous Pb^{2+} solutions with initial Pb concentrations of 10, 25, 50, 100, 250, 500, 750, and 1000 mg L^{-1} were prepared using lead(II) acetate as the Pb source. GDY powder (2.0 mg) was added to 2.0 mL of each Pb^{2+} solution, and the mixed solutions were stirred at room temperature for 24 hours. The GDY powder was then removed by centrifugation, and the supernatant was filtered through a 0.22-μm membrane filter. The remaining Pb concentration was quantified by ICP-MS, yielding equilibrium Pb concentrations of 0.0589, 0.2547, 1.0362, 4.0105, 8.9581, 104.8608, 307.1930, and 502.8390 mg L^{-1}, respectively, for the eight initial concentrations. The equilibrium sorption capacity (q_e) was calculated according to

$$q_e = \frac{(C_0 - C_e)V}{m} \quad (S3)$$

where C_0 and C_e are the initial and equilibrium Pb concentrations (mg L^{-1}), respectively, V is the solution volume (L), and m is the mass of GDY (g). The Langmuir-derived maximum sorption capacity (q_{max}) can be calculated by the linearized Langmuir relation:

$$\frac{C_e}{q_e} = \frac{1}{K_L q_{max}} + \frac{C_e}{q_{max}} \quad (S4)$$

where K_L is the Langmuir affinity constant (L mg^{-1}). The linearized Langmuir analysis

yielded a slope of 0.00197 g mg^{-1} and an intercept of 0.0459 g L^{-1}, corresponding to a Langmuir affinity constant (K_L) of 0.0429 L mg^{-1} and an apparent maximum Pb sorption capacity of 508 mg g^{-1} for GDY.

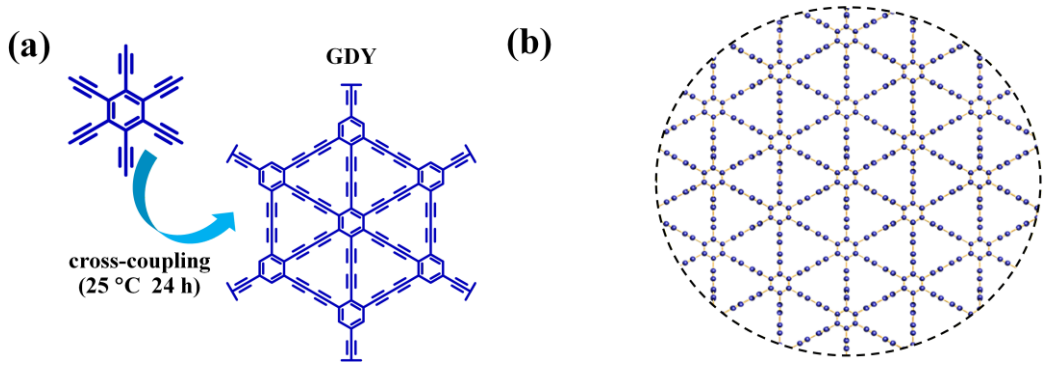

Supplementary Figure 1. (a) Diagram of the synthesis process of GDY; (b) Structure diagram of GDY.

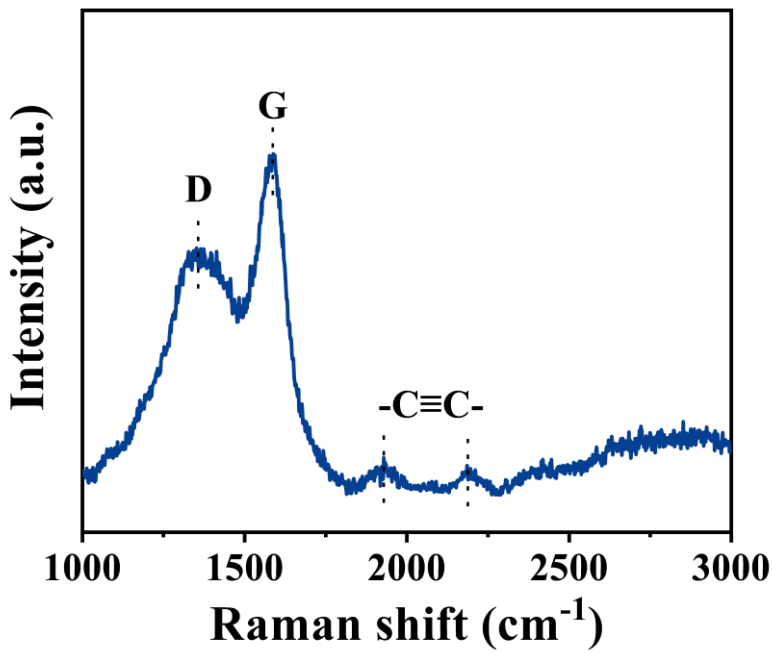

Supplementary Figure 2. Raman spectrum of GDY.

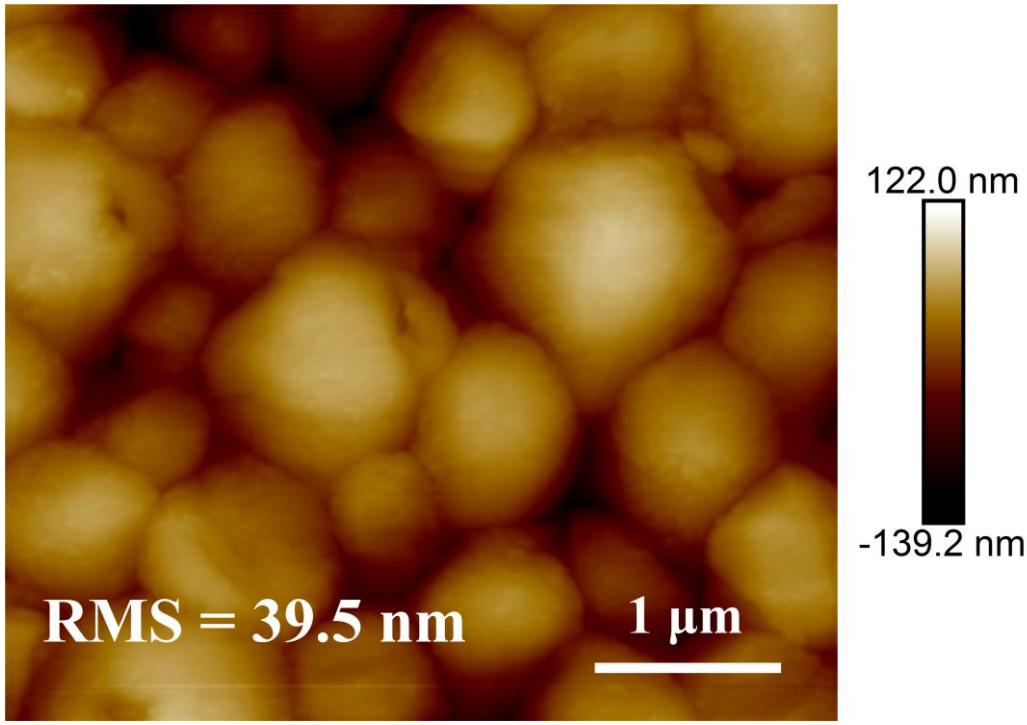

Supplementary Figure 3. AFM image of perovskite film.

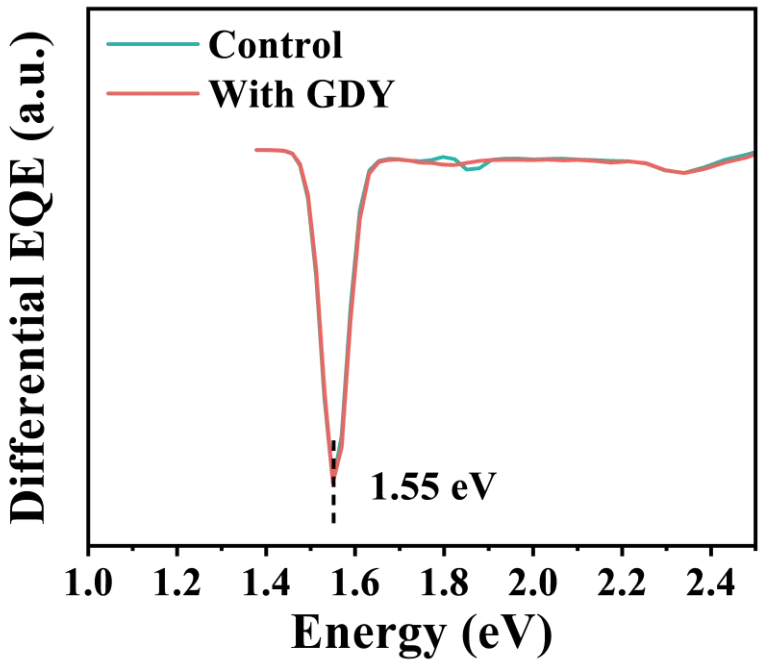

Supplementary Figure 4. The first derivative of EQE curves.

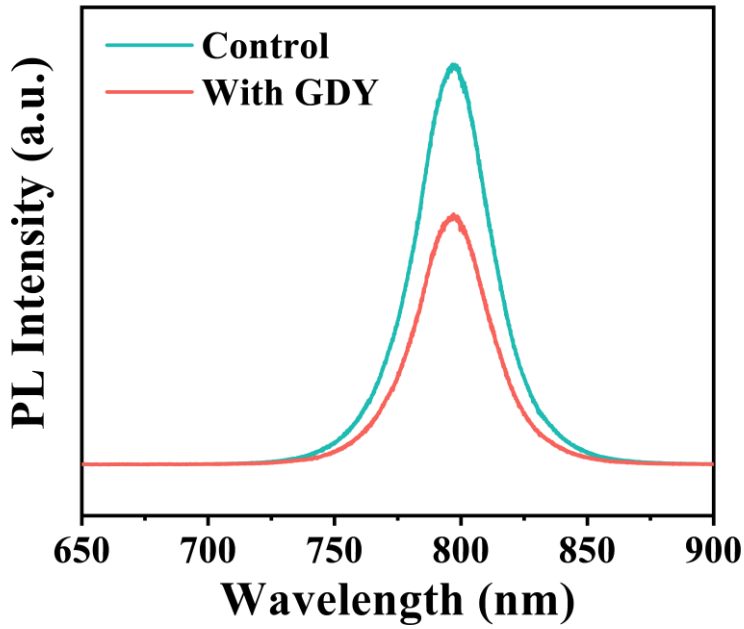

Supplementary Figure 5. Steady-state PL spectra for perovskite devices without and with GDY modification.

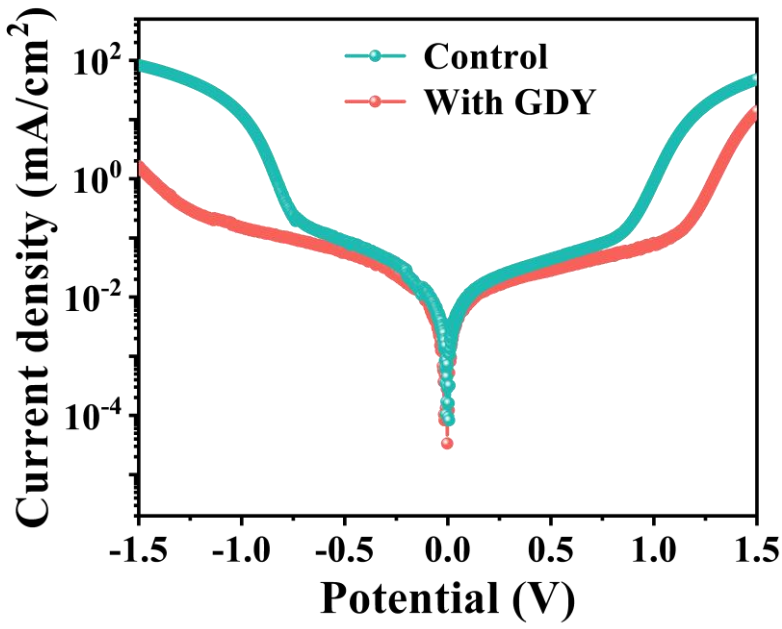

Supplementary Figure 6. Dark J-V curves of PSCs without and with GDY modification.

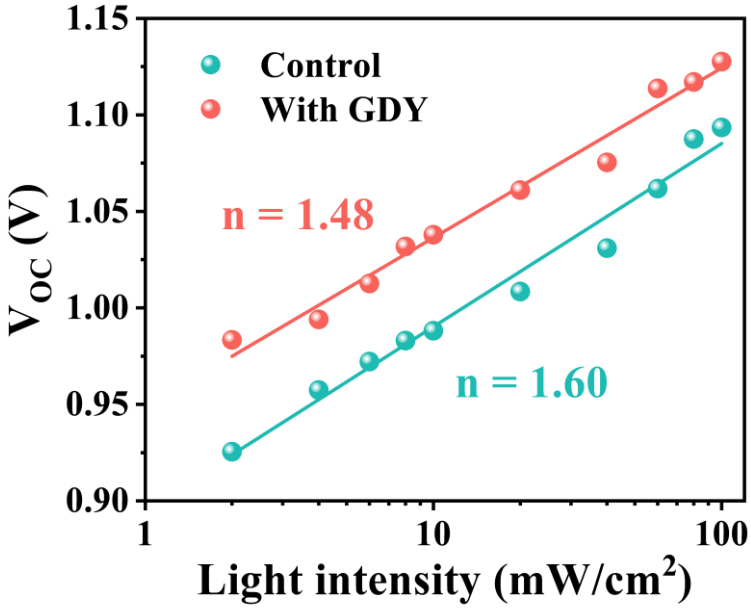

Supplementary Figure 7. V_{OC} as a function of light intensity for PSCs without and with GDY modification.

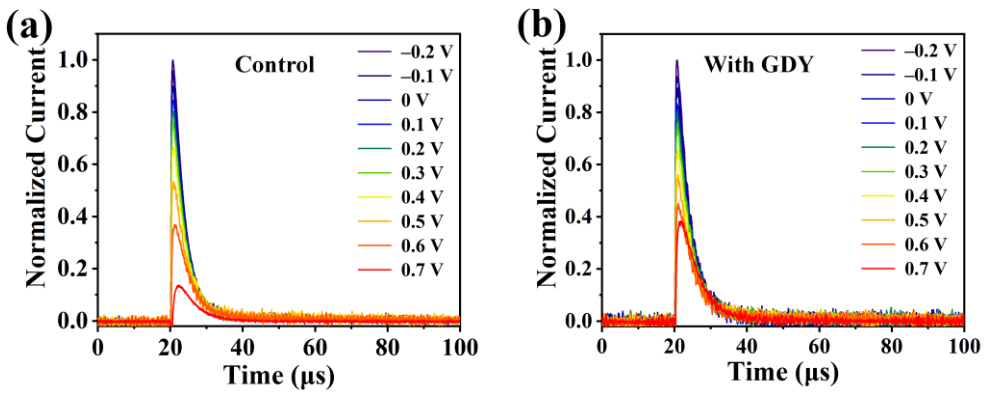

Supplementary Figure 8. Transient photocurrent (TPC) responses of PSCs (a) without and (b) with GDY modification under different bias voltages.

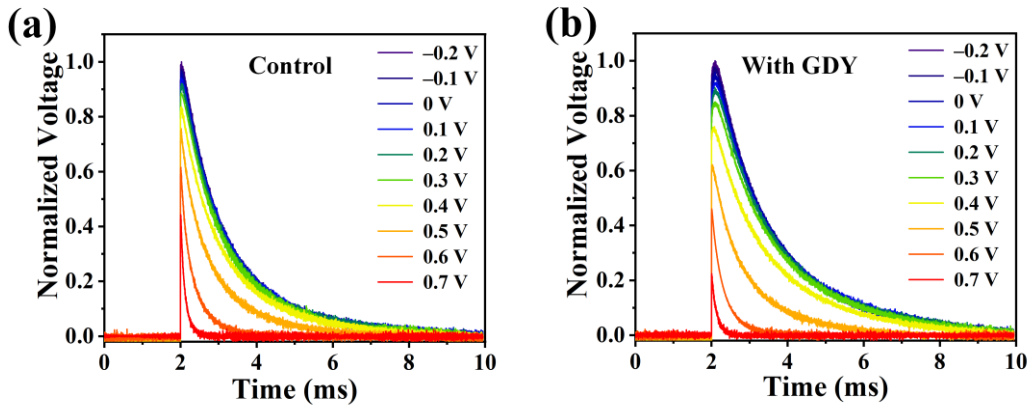

Supplementary Figure 9. Transient photovoltage (TPV) responses of PSCs (a) without and (b) with GDY modification under different bias voltages.

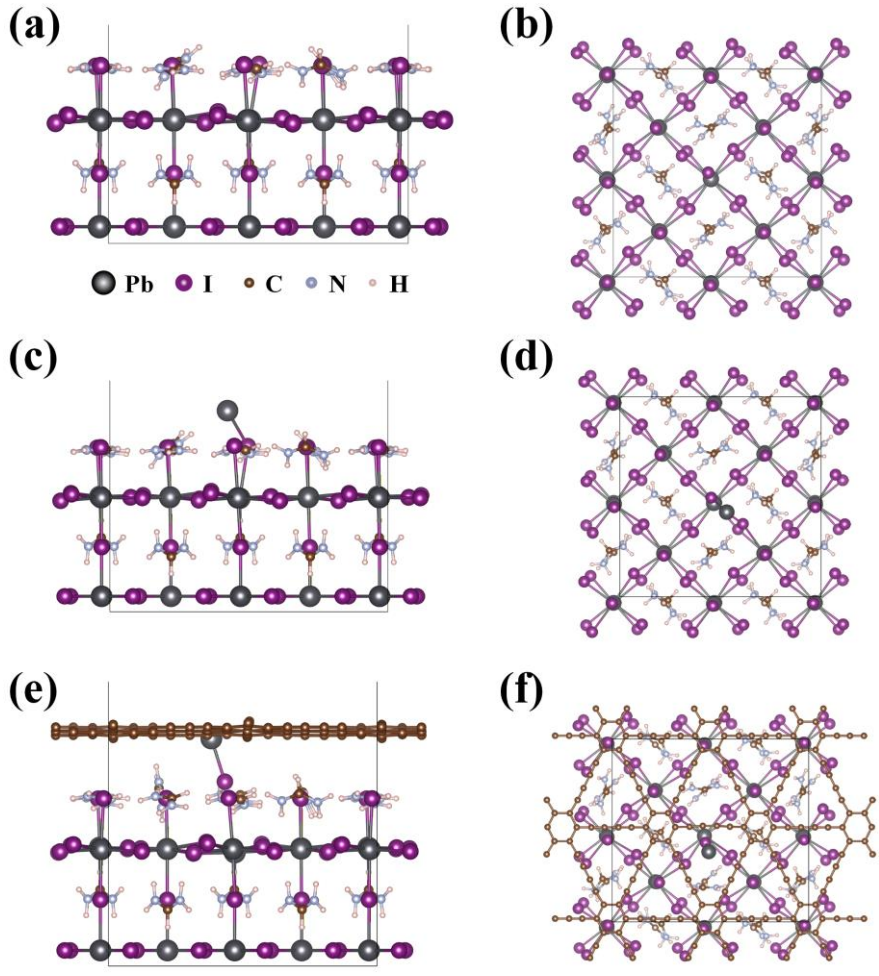

Supplementary Figure 10. Side view (left) and top view (right) of the optimized

structure: (a,b) pristine $FAPbI_3$ (001) surface; (c,d) $FAPbI_3$ (001) with an undercoordinated Pb^{2+} defect; (e,f) $FAPbI_3$ (001) with an undercoordinated Pb^{2+} defect and adsorbed GDY.

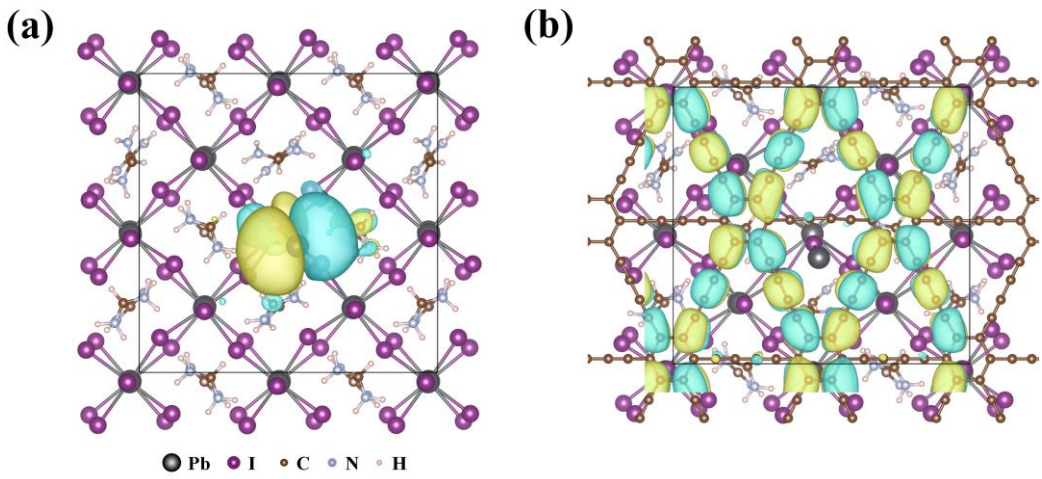

Supplementary Figure 11. Top views of the VBM Kohn-Sham wavefunction associated with the Pb-related defect state of the perovskite with (a) an undercoordinated Pb^{2+} defect and (b) the corresponding GDY-modified configuration. The black, purple, brown, cyan, and pink spheres indicate Pb, I, C, N, and H, respectively.

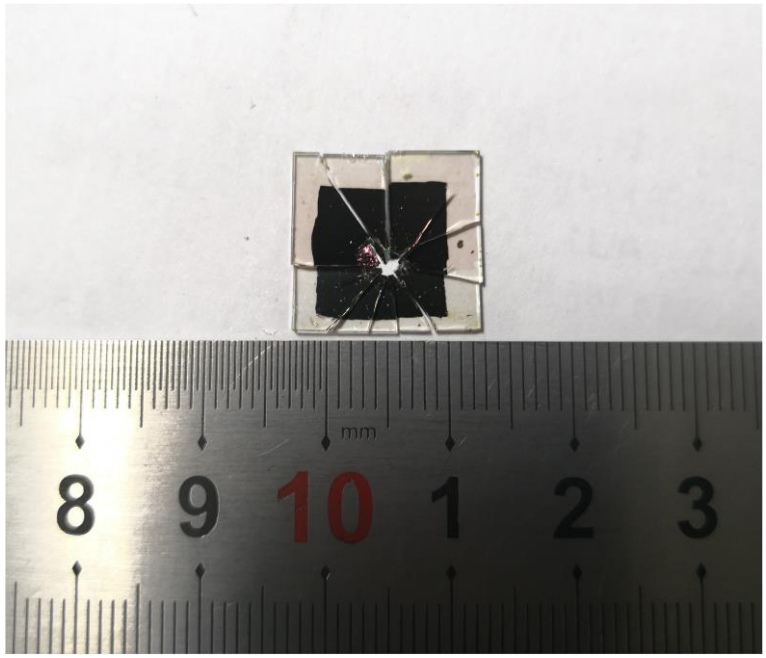

Supplementary Figure 12. Photograph of a mechanically fractured PSC used for the Pb-leakage test. This photograph was taken by the authors.

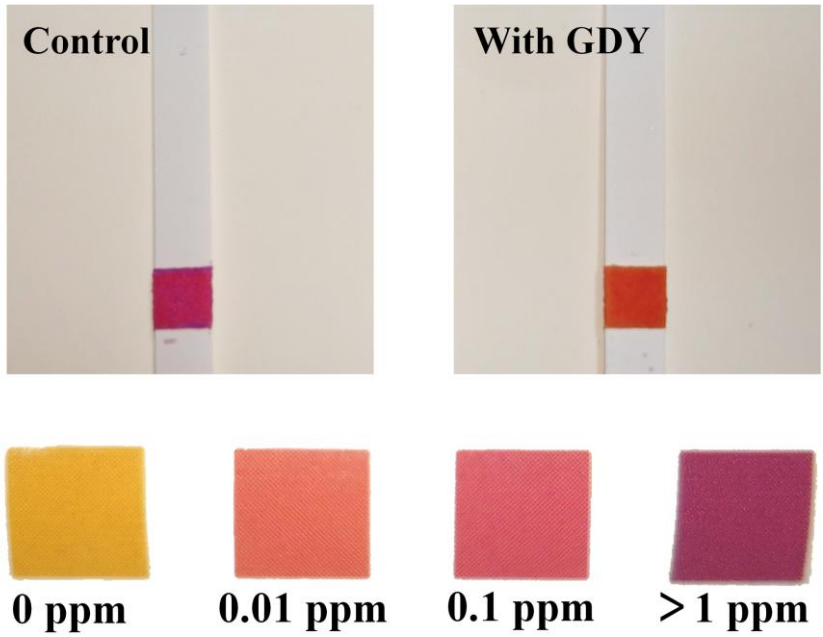

Supplementary Figure 13. Damaged PSCs without and with GDY were immersed in deionized water for 150 min, and Pb^{2+} test strips were used for rapid qualitative assessment of Pb concentration in the immersion solution.

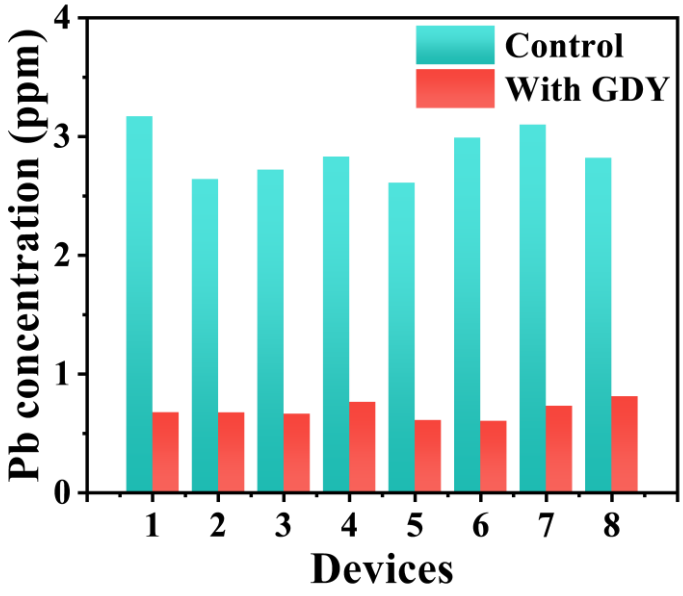

Supplementary Figure 14. Pb concentration measured for eight devices per condition after 150 min immersion in simulated acid rain (pH 4.5).

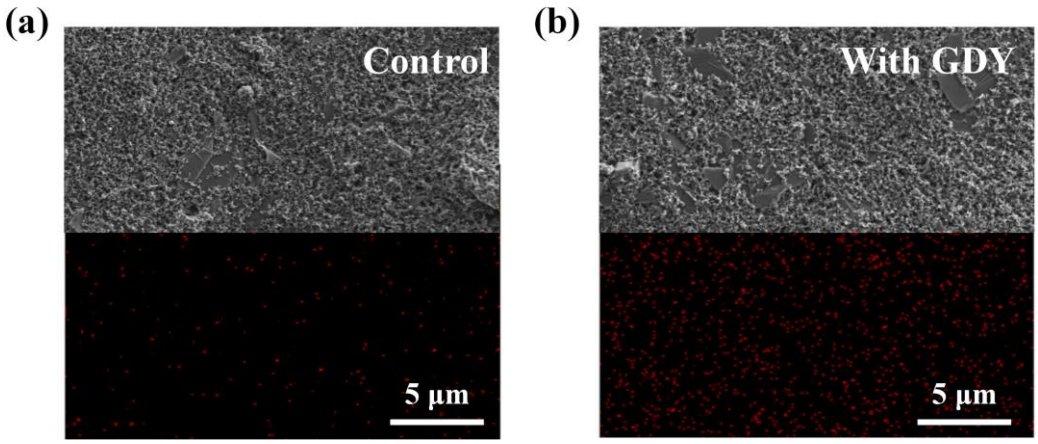

Supplementary Figure 15. SEM images (top) and corresponding EDS elemental maps of Pb (bottom) for (a) pristine carbon and (b) GDY-modified carbon films after immersion in a 10 ppm Pb^{2+} aqueous solution for 10 min. The red signals in the EDS elemental maps indicate the spatial distribution of Pb.

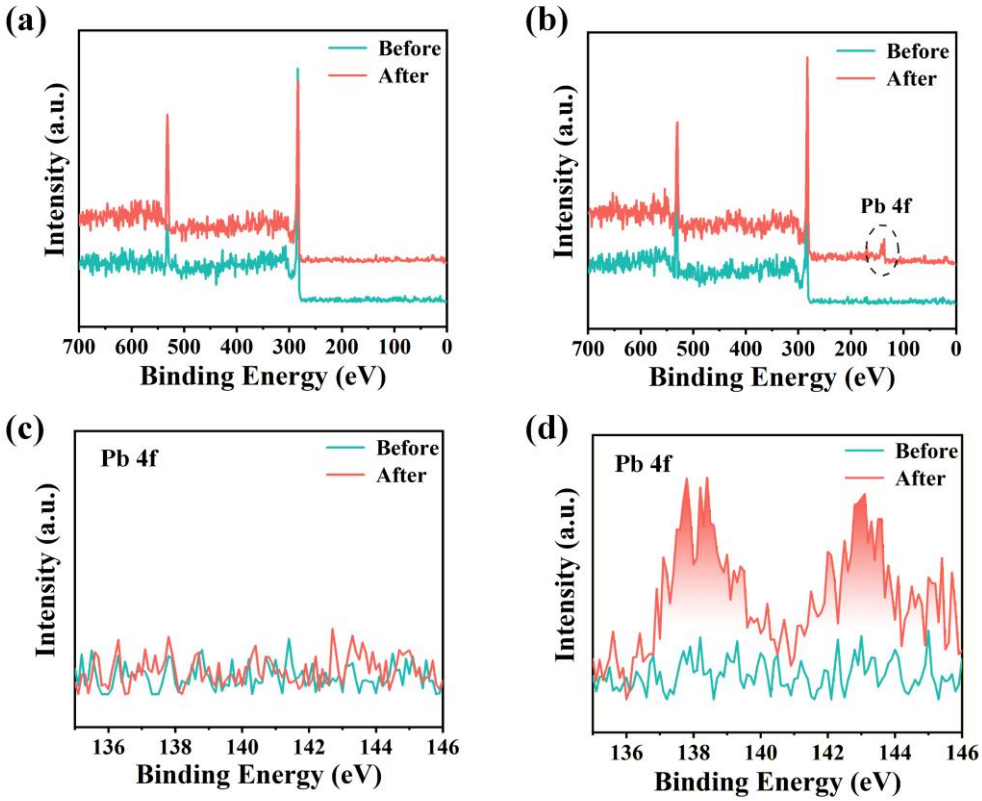

Supplementary Figure 16. XPS spectra of (a) pristine carbon film and (b) carbon: GDY film before and after immersion; High-resolution XPS Pb 4f spectra of (c) pristine carbon film and (d) carbon: GDY film before and after immersion.

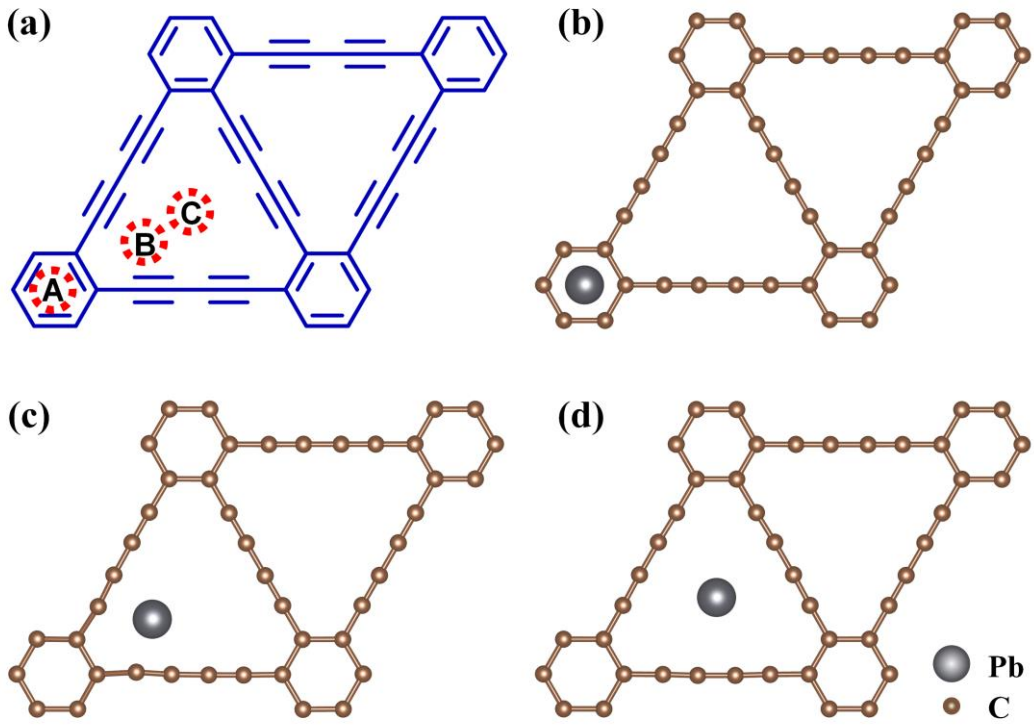

Supplementary Figure 17. (a) Representative adsorption sites for a single Pb atom on GDY: A, hollow site above the benzene-ring center; B, corner site of the acetylenic ring; and C, hollow site above the acetylenic-ring center; Optimized geometries for Pb adsorption at the (b) A, (c) B, and (d) C sites.

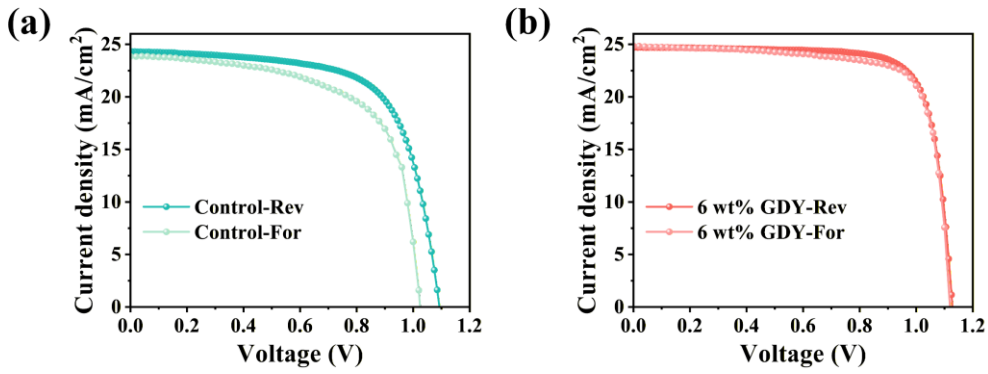

Supplementary Figure 18. Forward (For) and reverse (Rev) J-V curves for (a) control and (b) optimal GDY-modified devices under one-sun illumination.

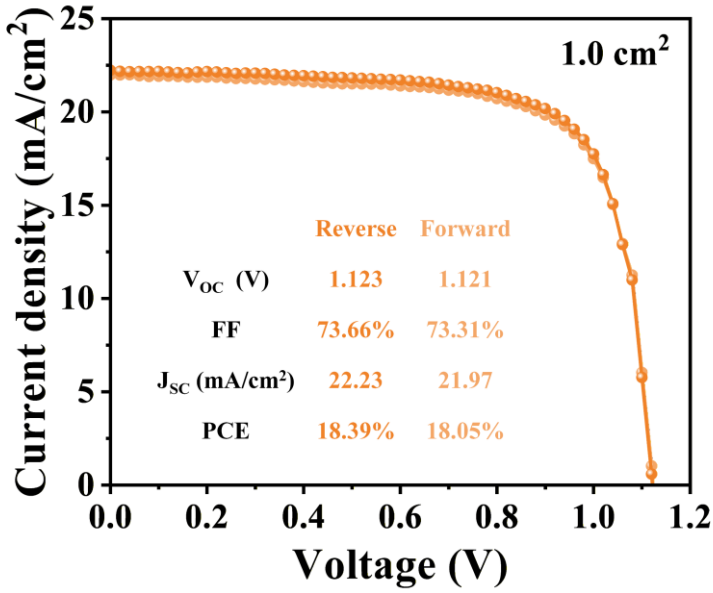

Supplementary Figure 19. J-V characteristics of 1 cm^2 champion PSCs for the GDY-modified carbon-based perovskite solar cells.

Supplementary Table 1. Fitting parameters based on biexponential decay function in TRPL spectrum

Sample	**A_1**	**A_2**	**τ_1/ns**	**τ_2/ns**	**τ_{avg}/ns**
Control	0.02	0.98	8.72	109.46	109.29
With GDY	0.06	0.94	8.57	64.21	63.74

The average decay time is calculated according to the equation:

$\tau_{\mathrm{avg}} = (A_1{\tau_1}^2 + A_2{\tau_2}^2)/(A_1\tau_1 + A_2\tau_2)$.

Supplementary Table 2. The fitting lifetimes derived from modulated transient photocurrent (μs)

Bias voltage (V)	**-0.2**	**-0.1**	**0**	**0.1**	**0.2**	**0.3**	**0.4**	**0.5**	**0.6**	**0.7**
Control	3.69	3.79	3.82	3.93	3.96	4.02	4.13	4.28	4.65	5.41
With GDY	3.32	3.38	3.41	3.42	3.54	3.59	3.63	3.86	4.01	5.21

Supplementary Table 3. The fitting lifetimes derived from modulated transient photovoltage (ms)

Bias voltage (V)	**-0.2**	**-0.1**	**0**	**0.1**	**0.2**	**0.3**	**0.4**	**0.5**	**0.6**	**0.7**
Control	1.15	1.17	1.18	1.18	1.20	1.19	1.16	0.72	0.30	0.12
With GDY	1.49	1.53	1.57	1.59	1.61	1.62	1.52	0.98	0.42	0.17

Supplementary Table 4. Calculated charge-collection efficiency (η_{coll}) and recombination rate (k_r) derived from TPC and TPV measurements under different bias voltages

Bias voltage (V)	**-0.2**	**-0.1**	**0**	**0.1**	**0.2**	**0.3**	**0.4**	**0.5**	**0.6**	**0.7**
Control-η_{coll} (%)	99.68	99.68	99.68	99.67	99.67	99.66	99.64	99.41	98.45	95.49
With GDY-η_{coll} (%)	99.78	99.78	99.78	99.78	99.78	99.78	99.76	99.61	99.05	96.94
Control-k_r (ms^{-1})	0.87	0.85	0.85	0.85	0.83	0.84	0.86	1.39	3.33	8.33
With GDY-k_r (ms^{-1})	0.67	0.65	0.64	0.63	0.62	0.62	0.66	1.02	2.38	5.88

Supplementary Table 5. The photovoltaic parameters derived from the *J-V* curves of PSCs with different amounts of GDY

Sample	**V_{OC}/V**	**J_{SC}/mA·cm^{-2}**	**FF**	**PCE**
Control	1.093	24.32	67.3%	17.89%
3 wt%	1.116	24.45	72.1%	19.67%
6 wt%	1.128	24.71	77.9%	21.71%
9 wt%	1.122	24.51	75.5%	20.76%

Supplementary Table 6. Parameters obtained from electrochemical impedance spectroscopy (EIS) fitting for different devices

	R_s (Ω)	R_{tr} (Ω)	CPE_{tr}-T	CPE_{tr}-P	R_{rec} (Ω)	CPE_{rec}-T	CPE_{rec}-P
Control	12.42	867	2.25 E-8	0.916	435	1.24 E-4	0.888
With GDY	12.70	673	2.30 E-8	0.914	899	1.01 E-4	0.839